

## An Accurate von Neumann's Law for Three-Dimensional Foams

Sascha Hilgenfeldt,<sup>1,\*</sup> Andrew M. Kraynik,<sup>2</sup> Stephan A. Koehler,<sup>1</sup> and Howard A. Stone<sup>1</sup>

<sup>1</sup>*Division of Engineering and Applied Sciences, Pierce Hall, Harvard University, Cambridge, Massachusetts 02138*

<sup>2</sup>*Engineering Sciences Center MS 0834, Sandia National Laboratories, Albuquerque, New Mexico 87185-0834*

(Received 15 September 2000)

The diffusive coarsening of 2D soap froths is governed by von Neumann's law. A statistical version of this law for dry 3D foams has long been conjectured. A new derivation, based on a theorem by Minkowski, yields an explicit analytical von Neumann's law in 3D which is in very good agreement with detailed simulations and experiments. The average growth rate of a bubble with  $F$  faces is shown to be proportional to  $F^{1/2}$  for large  $F$ , in contrast to the conjectured linear dependence. Accounting for foam disorder in the model further improves the agreement with data.

DOI: 10.1103/PhysRevLett.86.2685

PACS numbers: 82.70.Rr, 05.70.Ln, 68.90.+g

Researchers in diverse fields have studied foams for very different reasons [1]. Foams are viscoelastic "soft condensed matter" systems, with intriguing rheology [2] and drainage behavior [3]. They have numerous applications as detergents, lightweight structural materials, and in oil recovery [1]. Mathematicians have treated soap films as approximations to minimal surfaces, and soap froths as tessellations of space [4,5].

One physical process at work in a foam is *diffusive coarsening*, i.e., the growth of the average bubble size due to gas exchange between bubbles [6]. This process (also known as aging) is akin to Ostwald ripening [7,8], where large grains or droplets of condensed phase grow at the expense of smaller units by material diffusion through the continuous phase between them. The grains are usually treated as isolated and spherical, although corrections for closer proximity can be made [9]. In a *dry foam* (with little or no continuous phase), however, the bubbles touch and fill space, and therefore have *polyhedral* shape. Diffusion occurs through films of small thickness bounded by the faces of neighboring bubbles. In this case, bubble geometry and bubble configuration in the foam are important for the physical process of gas exchange.

In a dry two-dimensional foam, the bubbles are curved polygons. von Neumann showed [10] that the rate of area change  $\dot{a}$  of a given bubble is *independent* of its size, and solely dependent on its number of edges  $n$ ,

$$\dot{a} = D_2(n - n_0), \quad (1)$$

where  $D_2$  is an effective diffusion coefficient. The relation is strictly linear in  $n$ , and neutral growth (constant area) occurs for  $n_0 = 6$ . In three dimensions the evolution of the volume  $V$  of a polyhedral bubble is governed by [8]

$$V^{-1/3}\dot{V} = -D_{\text{eff}}V^{-1/3} \int_{\text{faces}} \mathcal{H} dA \quad (2)$$

with another effective diffusion coefficient  $D_{\text{eff}}$ . The growth rate is proportional to the integral of the mean curvature  $\mathcal{H}$  of the faces, as bubble growth at the expense of neighboring bubbles is driven by pressure differences

$\Delta p \propto \mathcal{H}$  (Young-Laplace law). By definition,  $\mathcal{H} > 0$  on convex faces, which favor bubble shrinkage ( $\dot{V} < 0$ ).

A realistic foam consists of a random distribution of bubbles of many different shapes and sizes (see Fig. 1a), so that the integral in (2) varies with the individual bubble geometry. Averaging over all shape variations of polyhedral bubbles with  $F$  faces (" $F$ -bubbles"), one arrives at

$$V_F^{-1/3}\dot{V}_F = D_{\text{eff}}\mathcal{G}(F) \equiv -D_{\text{eff}}V_F^{-1/3} \left\langle \int_{\text{faces}} \mathcal{H} dA \right\rangle_F, \quad (3)$$

a statistical von Neumann-like law, where  $\langle \cdot \rangle_F$  is the average over  $F$  bubbles, and  $V_F = \langle V \rangle_F$ . Attempts to determine the dimensionless function  $\mathcal{G}$  have included a maximum-entropy formalism [11], Potts model simulations [12], numerical calculations for idealized froths [13,14], and experiments [15]. All conclude that there is a face number  $F_0$  where  $\mathcal{G}(F_0) = 0$ , and that  $\mathcal{G}(F)$  is approximately or exactly linear around  $F_0$  [11]. Numerical values for  $F_0$  range from 13.4 [15] to 15.8 [12]. In this Letter, we derive an analytical expression for  $\mathcal{G}(F)$ .

In 1903, Minkowski [16] related the volume, surface area, and mean curvature of convex bodies to a quantity we call the *caliper radius*  $C(\theta, \varphi)$ , cf. [17]. Fix a spherical coordinate system at an origin  $O$  inside the body and draw a plane normal to the spatial direction  $(\theta, \varphi)$  through  $O$ . Then,  $C(\theta, \varphi)$  is the maximum distance between this plane and any parallel plane touching the body (Fig. 1b). Minkowski showed that

$$\int_{4\pi} C(\theta, \varphi) d\omega = \int_{S_K} \mathcal{H} dA \quad (4)$$

for any convex body  $K$ , where the integrals are over all solid angles ( $d\omega = \sin\theta d\theta d\varphi$ ) and the total surface area  $S_K$  of  $K$ , respectively. If  $K_0$  is a polyhedron with *flat* faces, the mean curvature is localized in the edges. By replacing the sharp edges by cylindrical sections of infinitesimal radius, (4) can be evaluated explicitly to obtain

$$\int_{4\pi} C_0(\theta, \varphi) d\omega = \int_{S_{K_0}} \mathcal{H} dA = \sum_{i=1}^E \frac{1}{2} \chi_i L_i, \quad (5)$$

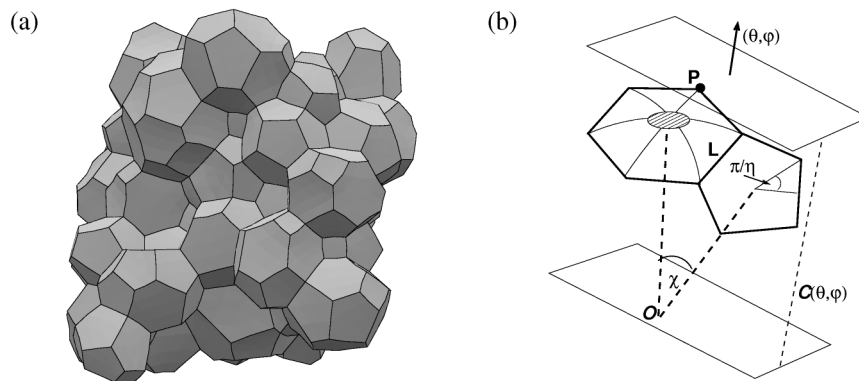


FIG. 1. (a) Example of a surface evolver simulation of a spatially periodic poly-disperse dry foam with 64 bubbles. (b) Schematic of two adjacent polygonal faces on a polyhedral foam bubble with centroid  $O$ . The two planes are perpendicular to the direction  $(\theta, \varphi)$ ; the upper one touches the body at the vertex  $P$ . Their distance is  $C(\theta, \varphi)$ . The shaded area illustrates the  $\mathcal{O}(L^2/R^2)$  fraction of spatial directions for which  $C(\theta, \varphi)$  on the curved face differs from its value for a flat face (see text;  $R$  is the radius of curvature of the face).

where  $E$  is the number of edges on  $K_0$ , and  $\chi_i$  is the angle between adjacent face normals (see Fig. 1b), i.e., the complement of the dihedral angle between the faces that shares an edge of length  $L_i$ .

Dry foam bubbles are polyhedra with gently curved faces, i.e., part of the mean curvature resides in the faces,

$$\int_{4\pi} C(\theta, \varphi) d\omega = \int_{\text{faces}} \mathcal{H} dA + \sum_{i=1}^E \frac{\pi}{6} L_i. \quad (6)$$

We have made use of Plateau's rule [4] which enforces dihedral angles of  $2\pi/3$  locally at every edge of a foam bubble. The localized curvature at the edges can therefore be evaluated by replacing all  $\chi_i$  by  $\pi/3$ .

We now compare a foam bubble  $K$  and its "skeleton" polyhedron  $K_0$ , obtained by replacing the curved faces by (piecewise) flat faces spanned between the vertices of  $K$ . Following Sire [13], we idealize the curved surfaces of  $K$  to be spherical caps of radius  $R \gg L$ , where  $L \sim L_i$  is a typical edge length. Then, the caliper radii of both  $K$  and  $K_0$  can be calculated analytically to leading order in  $L/R$ . For  $K_0$ ,  $C(\theta, \varphi) = C_0(\theta, \varphi)$  is determined by a plane through a vertex  $P$  (see Fig. 1b) for all  $(\theta, \varphi)$ . For  $K$ , this is still true for most directions, with the exception of an  $\mathcal{O}(L^2/R^2)$  fraction of solid angles around the direction of each face normal (shaded region in Fig. 1b). The actual difference between  $C$  and  $C_0$  for those  $(\theta, \varphi)$  is of order  $L^2/R$  (the orders do not depend on the specific spherical shape of the caps chosen). Therefore,

$$\int_{4\pi} C(\theta, \varphi) d\omega - \int_{4\pi} C_0(\theta, \varphi) d\omega = L\mathcal{O}[(L/R)^3], \quad (7)$$

i.e., the two integral caliper radii are equal up to second order in  $L/R$ . Equation (7) is valid for bubbles with concave faces as well, when in the definition of  $C(\theta, \varphi)$  the outer plane is forced to touch the bubble on the inwardly curved surface for central solid angles. Thus, (6) is applicable to all foam bubbles, cf. the proof of (4) in [17]. By using (5)–(7) we find, to second order in  $(L/R)$ ,

$$\int_{\text{faces}} \mathcal{H} dA = \sum_{i=1}^E \frac{1}{2} \left( \chi_i - \frac{\pi}{3} \right) L_i. \quad (8)$$

Note that this formula applies to each individual bubble, whose integral mean curvature (and therefore coarsening

rate) is determined by the dihedral angles of its polyhedral skeleton alone. To find  $\mathcal{G}(F)$ , an average over all  $F$ -bubbles is necessary. The easiest and most idealized model is to assume that all  $F$ -bubbles are identical regular polyhedra, having a single type of regular curved face with  $\eta_F$  edges and equal edge lengths  $L_F$ . From Euler's and Plateau's laws, we get  $E = 3F - 6$  and  $\eta_F = 6 - 12/F$ , and, from the geometry of the regular polyhedron (every face subtends a solid angle of  $4\pi/F$ ), one finds

$$\chi_F = 2 \arctan[(4 \sin^2(\pi/\eta_F) - 1)^{1/2}]. \quad (9)$$

Demanding  $\chi_F = \pi/3$  for the nongrowing bubble, we obtain  $F_0^* = 12/(6 - \pi/\arcsin\sqrt{1/3}) = 13.397\dots$ , a well-known value conjectured to be the average face number in a minimal-area foam with equal pressure bubbles [5,18]. A hypothetical regular bubble with  $F = F_0^*$  would have all flat surfaces and still fulfill Plateau's rules. Obviously, noninteger  $F$  cannot exist, but treating  $F$  as a real number gives insight into the statistical properties of a foam.

The edge length  $L_F$  of a regular  $F$ -bubble of volume  $V$  is determined to leading order in  $L/R$  by equating  $V$  to the volume of the polyhedral skeleton. Combining the result with (3) and (8), the growth function  $\mathcal{G}(F)$  is found explicitly and analytically, without free parameters, as

$$\mathcal{G}(F) = \frac{3[(F - 2) \tan \frac{\pi}{\eta_F}]^{2/3} \tan^{1/3}(\frac{\chi_F}{2})}{2^{1/3}} \left( \frac{\pi}{3} - \chi_F \right). \quad (10)$$

With (3), this yields an analytical 3D von Neumann law. The result improves on previous work [13], in that it does not need distributions of face numbers and solid angles as input parameters, and yields very good agreement with observed growth rates and measured  $F_0$  in actual foams [15] as well as in detailed simulations of random foams. The latter were performed with the surface evolver [19] and consider up to 1000 bubbles with periodic boundary conditions, thus avoiding artifacts of peripheral bubble geometry [14,20]. The structures (see Fig. 1a) are carefully relaxed to a stationary state (local minimum of surface area). These simulations do not include gas diffusion between bubbles, but instead register the pressure differences  $\Delta p$ , allowing us to calculate  $\mathcal{G}(F)$ . The symbols in

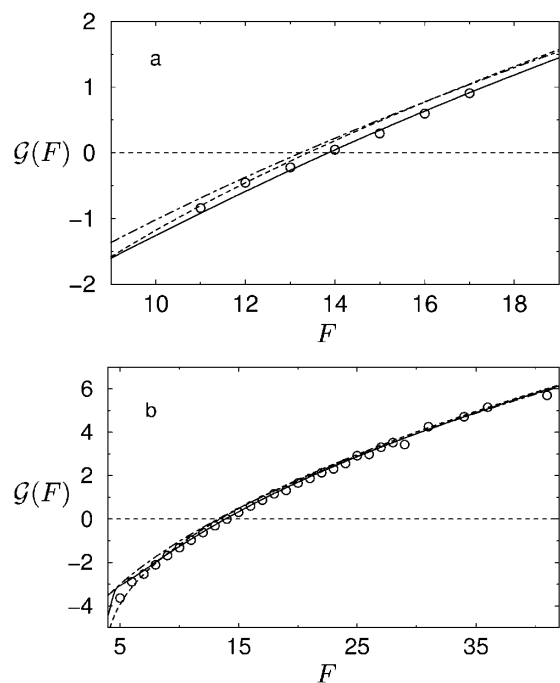


FIG. 2. The growth function  $\mathcal{G}(F)$  of a random foam from surface evolver simulations (circles) and from theory. The simulations are for 512 monodisperse bubbles (a) and 512 strongly polydisperse bubbles (b) with a log-normal volume distribution whose width in  $(\log V)$  space is  $\sigma_V \approx 0.86$ . Simulation error bars are smaller than the symbol size. The dashed and dot-dashed lines are the analytical formula (10) and its large- $F$  asymptote (11). The solid line includes corrections due to the distributions of edge numbers and edge lengths on the bubbles characterized by  $\sigma_\eta = 0.73$  (see text).

Fig. 2 stem from simulations for (a) monodisperse (equal-volume) and (b) polydisperse structures. The dashed line is the analytical formula (10), which does not distinguish between the mono- and polydisperse cases. Equation (10) is surprisingly accurate over the whole range of  $F$  in the simulations, with typical deviations of about 10%. The relative errors become larger, though, around  $F_0$  (Fig. 2a). Also, the simulated growth rates are somewhat smaller than the analytical ones, with  $F_0 \approx 13.82$  (monodisperse) and  $F_0 \approx 14.00$  (polydisperse) instead of  $F_0^*$ . While  $\mathcal{G}(F)$  is approximately linear in the limited range of  $F$  in the monodisperse case, the function is clearly nonlinear over the larger  $F$  range in polydisperse foams (Fig. 2b). The asymptote of (10) for large  $F$  is

$$\mathcal{G}(F \gg 1) = \frac{\pi^{7/6}}{2^{1/6} 3^{5/12}} F^{1/2} - 6^{1/3} 2\pi^{2/3}, \quad (11)$$

i.e., a *square-root* behavior, which is depicted as a dot-dashed line in Fig. 2. In the figure, it is indistinguishable from the full analytical expression (10) for  $F \gtrsim 15$ . The conjectured *linear* 3D von Neumann law [11,12] does not agree with the simulations. A square-root growth law for large  $F$  is implicit in the model of Ref. [14], which, however, shows substantial discrepancies to simulations.

We now consider a more realistic model foam, dropping the assumption of identical  $F$ -bubbles and allowing

for *disorder* by (i) introducing a distribution of regular polygonal faces with different edge numbers  $\eta$ , and (ii) letting the edge length vary with  $\eta$  ( $L_F \rightarrow L_{F,\eta}$ ). A random foam must inevitably have a variety of edge numbers, for which experiments [21] and simulations [22] give a distribution function well approximated by a Gaussian  $f(\eta) = \exp[-(\eta - \eta_F)^2/2/\sigma_\eta^2]/(2\pi)^{1/2}/\sigma_\eta$  with  $\sigma_\eta \approx 0.59$  [21] and 0.73 [22], respectively.

The  $\eta$  dependence of  $L$  allows the foam to reduce its surface area. We attempt to minimize the surface area  $A_F$  of the  $F$ -faced bubbles separately for each  $F$ , while keeping the volume  $V$  constant. Approximating  $A_F$  and  $V$  by their skeleton values, the minimization problem is

$$\delta A_F = \delta \int \frac{F\eta}{4 \tan(\pi/\eta)} f(\eta) L_{F,\eta}^2 d\eta = 0$$

with

$$V = \int \frac{F\eta}{12 \tan(\pi/\eta)} f(\eta) \tilde{h} L_{F,\eta}^3 d\eta = \text{const}, \quad (12)$$

where  $\tilde{h}$  is given by

$$\tilde{h} = \frac{1}{2 \sin \frac{\pi}{\eta}} \frac{\tan(\frac{\pi-\omega/2}{\eta})}{[\tan^2 \frac{\pi}{\eta} - \tan^2(\frac{\pi-\omega/2}{\eta})]^{1/2}}. \quad (13)$$

The solid angle  $\omega$  subtended by an  $\eta$ -edged face is approximated by the quotient of its area and the total bubble area at fixed edge length, i.e.,  $\omega = [\pi\eta/F \tan(\pi/\eta)]/[\int \eta' f(\eta')/(4 \tan(\pi/\eta')) d\eta']$ . The resultant optimum  $L_{F,\eta}$  is calculated to be

$$L_{F,\eta} = \frac{2V^{1/3}}{\lambda \tilde{h}},$$

with

$$\lambda = \left[ \int \frac{2F\eta f(\eta)}{3 \tan(\pi/\eta) \tilde{h}^2} d\eta \right]^{1/3}. \quad (14)$$

The angles  $\chi$  are altered by the  $\eta$  dependence as well to  $\chi_{F,\eta} = 2 \arctan\{1/[2\tilde{h} \tan(\pi/\eta)]\}$ .

In a final step,  $L_{F,\eta}$  is modified again because the foam bubbles are curved and some of the volume  $V$  resides in the spherical caps. To leading order, this changes edge lengths by  $-\Delta/(2\tilde{h})$ , where  $\Delta = L_{F,\eta}[1 - (1 - (\chi_{F,\eta} - \pi/3)^2/4)^{1/2}]/[\tan(\pi/\eta)(\chi_{F,\eta} - \pi/3)]$ . These edge lengths and angles, weighted by  $f(\eta)$  with  $\sigma_\eta = 0.73$ , yield the corrected growth function  $\mathcal{G}(F)$ , displayed as solid line in Fig. 2. The accuracy is improved to typically 2%-3%, and we obtain  $F_0 \approx 13.85$  (13.82 in the monodisperse simulations) with an error smaller than the statistical error in the simulations. The difference from  $F_0 = 14.00$  for the polydisperse system is significant and could stem from an effect of volume-face number correlations (bubbles with large volume tend to have many faces [23]). Larger deviations occur for the lowest  $F \approx 5$ , where interfaces are often strongly curved and the assumption  $R \gg L_{F,\eta}$  fails. Allowing for distributions of  $L$  at fixed  $F$ ,  $\eta$  could further refine the model. However, simulations suggest that these distributions are fairly narrow.

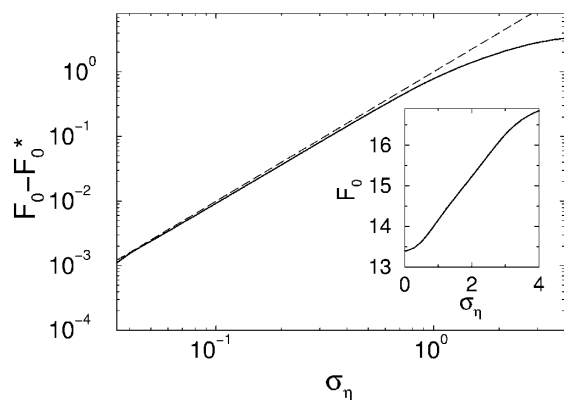


FIG. 3. Theoretical dependence of the neutral growth face number  $F_0$  on the width  $\sigma_\eta$  of the edge number distribution  $f(\eta)$  (solid line). The inset shows  $F_0(\sigma_\eta)$  on a linear scale, and the main figure indicates, as a dashed line, the quadratic power law for small  $F_0 - F_0^*$ .

Our values for  $F_0$  are smaller than those calculated with a Potts model [12], indicating larger disorder in that model. In foams, the time scale for the change of surface area via shape rearrangement is much smaller than that for area change by diffusive loss or gain of gas. This time scale separation is not present in the Potts model, i.e., the foam cannot relax to minimal surface area in every time step, which would anneal some of the disorder.

Matzke [21] did not consider gas diffusion or record  $F_0$  for his experimental foams, but gave the average face number  $\bar{F} \approx 13.70$ . As his structures were monodisperse, we expect  $\bar{F} = F_0$  [23]. Setting  $\sigma_\eta$  to Matzke's value (0.59) in our model gives  $F_0 \approx 13.70$ , in agreement with experiment. Figure 3 shows the computed variation of  $F_0$  with  $\sigma_\eta$ . As  $\sigma_\eta \rightarrow 0$ ,  $F_0^*$  is approached quadratically.

The simulations as well as the formalism presented here find that in a monodisperse foam the average area of  $F$ -bubbles increases with  $F$ , so that a minimal-area monodisperse foam is prone to have  $F_0 = \bar{F}$  as small as possible. As  $F_0$  grows with  $\sigma_\eta$ , the "optimal" foam must have a small  $\sigma_\eta$ . The inevitable presence of 4-, 5-, and 6-sided faces in a random foam, however, sets a lower limit to  $\sigma_\eta$ . Simple estimates [24] suggest  $\bar{F} \geq 13.6$  for unimodal  $F$  distributions. Only regular foams such as the Weaire-Phelan foam, currently the tessellation of space with the smallest surface area known [25], seem to approach  $\bar{F}$  as low as 13.5 [5].

The model presented here has yielded accurate growth rates throughout the range of bubble face numbers in realistic foams. Combined with number and volume distributions of  $F$ -bubbles in aged, statistically self-similar foams [8], macroscopic coarsening rates can be computed. The growth of  $\bar{F}$  with  $\sigma_\eta$  in monodisperse foams may give valuable clues in the attempt to solve Kelvin's problem of the optimal partition of space into equal volumes, whose solution has so far eluded researchers.

We thank Doug Reinelt for countless discussions. Kenneth Brakke's development of the surface evolver was

crucial to this work, and is gratefully acknowledged, as is grant support from the ACS-PRF fund and the Harvard MRSEC. Sandia is a multiprogram laboratory operated by Sandia Corporation, a Lockheed Martin Company, for the U.S. Department of Energy under Contract No. DE-AC04-94AL85000.

\*Present address: Applied Physics, University of Twente, P.O. Box 217, 7500 AE Enschede, The Netherlands.

Email address: sascha@tn.utwente.nl

- [1] J. J. Bikerman, *Foams* (Springer, New York, 1973); *Foams, Theory, Measurements and Applications*, edited by R. K. Prud'homme and S. A. Khan (Marcel Dekker, New York, 1996); D. Weaire and S. Hutzler, *The Physics of Foams* (Oxford University Press, Oxford, 2000).
- [2] A. M. Kraynik, *Annu. Rev. Fluid Mech.* **20**, 325 (1988).
- [3] G. Verbist, D. Weaire, and A. Kraynik, *J. Phys. Condens. Matter* **8**, 3715 (1996); S. A. Koehler, S. Hilgenfeldt, and H. A. Stone, *Phys. Rev. Lett.* **82**, 4232 (1999); S. A. Koehler, S. Hilgenfeldt, and H. A. Stone, *Langmuir* **16**, 6327 (2000).
- [4] J. A. F. Plateau, *Statique expérimentale et théorique des liquides soumis aux seules forces moléculaires* (Gauthier-Villars, Trubner et cie, Paris, 1873).
- [5] *The Kelvin Problem*, edited by D. Weaire (Taylor & Francis, London, 1996).
- [6] D. J. Durian, D. A. Weitz, and D. J. Pine, *Phys. Rev. A* **44**, R7902 (1991).
- [7] J. A. Marquee and J. Ross, *J. Chem. Phys.* **79**, 373 (1983).
- [8] W. W. Mullins, *J. Appl. Phys.* **59**, 1341 (1986).
- [9] S. P. Marsh and M. E. Glicksman, *Acta Mater.* **44**, 3761 (1996).
- [10] J. von Neumann, in *Metal Interfaces* (American Society for Metals, Cleveland, 1952), p. 108.
- [11] N. Rivier, *Philos. Mag. B* **47**, 91 (1983).
- [12] J. A. Glazier, *Phys. Rev. Lett.* **70**, 2170 (1993).
- [13] C. Sire, *Phys. Rev. Lett.* **72**, 420 (1994).
- [14] C. Monnerneau, N. Pittet, and D. Weaire, *Europhys. Lett.* **52**, 361 (2000).
- [15] C. Monnerneau and M. Vignes-Adler, *Phys. Rev. Lett.* **80**, 5228 (1998).
- [16] H. Minkowski, *Math. Ann.* **57**, 447 (1903).
- [17] M. G. Kendall and P. A. P. Moran, *Geometrical probability* (Griffin, London, 1963).
- [18] N. Rivier, *J. Phys. (Paris), Colloq.* **43**, C91 (1982).
- [19] K. Brakke, *Exper. Math.* **1**, 141 (1992).
- [20] S. Ross, *Am. J. Phys.* **46**, 513 (1978).
- [21] E. Matzke, *Am. J. Bot.* **33**, 58 (1946).
- [22] A. M. Kraynik, D. A. Reinelt, and F. van Swol, in *Proceedings of the 3rd EuroConference on Foams, Emulsions and Applications*, edited by P. Zitha (MIT-Verlag, Bremen, 2000).
- [23] D. Weaire and J. A. Glazier, *Philos. Mag. Lett.* **68**, 363 (1993).
- [24] S. Hilgenfeldt, A. Kraynik, S. A. Koehler, and H. A. Stone (unpublished).
- [25] D. Weaire and R. Phelan, *Nature (London)* **367**, 123 (1994).